AI-based blood pressure estimation from photoplethysmography signals to develop medical monitoring devices' capabilities

Seyedehsamaneh Shojaeilangari[١,*], Masume Khaleghian[٢], Maryam Beigzadeh[١]

[١] **Biomedical Engineering group, Department of Electrical and Information Technology, Iranian Research Organization for Science and** *Technology (IROST), 33535111, Tehran, Iran*

[٢] **Department of Electrical and Computer Engineering, Faculty of Artificial Intelligence, Kharazmi University, Tehran, Kara, Iran.**

[*] *Corresponding author: Seyedehsamaneh Shojaeilangari, E-mail: s.shojaie@irost.ir*

Abstract

Accurate estimation of blood pressure (BP) is critical for managing and preventing cardiovascular diseases. Traditional cuff-based methods, such as auscultatory and oscillometric monitors, require cumbersome devices that often cause patient's discomfort. Recent advancements in wearable technologies have enabled the non-invasive monitoring of BP using photoplethysmogram (PPG) signals. This study proposes an artificial intelligence (AI) framework including a deep supervised multi-residual U-Net (DSMR-UNet) architecture for the prediction of arterial BP (ABP) waveform and the estimation of systolic/diastolic BP from PPG signal. Comprehensive analyses were conducted on two databases, one of which is part of a publicly available standard dataset (so-called UCI), and the other is a native dataset developed for this project. Our experimental findings demonstrate the impressive efficacy of the proposed method, where we achieved mean absolute errors (MAE) of ٤,٣٤ and ٣,٣٢, and standard deviations (STD) of ٥,٦٣ and ٤,٦٣, respectively, for systolic and diastolic BP on the UCI database. Our performance was acknowledged with a grade of A in the British Hypertension Society (BHS) standard and satisfied the criteria for the Association for the Advancement of Medical Instrumentation (AAMI). It is worth mentioning that to examine the generalization power of the proposed method, it was tested on the native dataset, achieving MAE of ١٦,٣٣ and ٧,٤٥, and STD of ١٢,٣٢ and ٦,٤٤, respectively, for systolic and diastolic BP. According to this study, the suggested AI framework shows promise for estimating blood pressure using PPG signals for real-world applications .

Keywords

Blood pressure, Cuff-less estimation, Photoplethysmography, Deep learning, Non-invasive, Artificial intelligence

١ Introduction

Photoplethysmography (PPG) is a non-invasive, cost-effective, and simple approach for detecting alterations in blood volume within the microvascular bed of tissues. PPG signals are frequently utilized in wearable devices to estimate heart rate, oxygen saturation levels, and other vital signs. Recent research studies have focused on the potential applicability of PPG signals to estimate BP, providing a continuous, comfortable, and convenient method for BP monitoring. PPG signals are typically obtained using a light-emitting diode (LED) and a photodiode detector that measures changes in light absorption due to blood flow through the vessels. When blood pressure increases, blood flow and light absorption also increase. Consequently, the shape and amplitude of the PPG waveform change and provide potential indicators for BP.

Several studies have demonstrated relationships between specific PPG waveform characteristics and BP. For example, some studies suggest a correlation between the time difference of systolic peaks in PPG or

ECG signals and BP (so-called pulse transit time (PTT)) [١]. Some others have noted a relationship between the PPG waveform's features (like amplitude or area) and BP [٢].

In general, BP estimation algorithms from PPG signals follow a two-step process: feature extraction and BP prediction. The first step involves extracting representative features from the PPG signals. These features may comprise time-domain attributes (e.g., peak-to-peak interval, PTT) [٣], frequency-domain features (e.g., power spectral density) [٤], and morphological ones (e.g., waveform amplitude, area) [٥]. The second step involves correlating the extracted features with BP values. Simple linear regression is the most common method used [٦]. However, due to the non-linear and non-stationary nature of PPG and BP signals, more complex models such as multiple regressions, neural network models, and machine learning (ML) models [٢], [٧], [٨] have been proposed. Recent advances in the artificial intelligence (AI) community have shown great promise in applying deep learning (DL) for regression or classification problems [٩]–[١١]. DL techniques, especially convolutional neural networks (CNNs), have demonstrated their effectiveness in many medical signal-processing tasks by automatically learning representations directly from raw data [١٠], [١٢], [١٣].

In recent years, there has been a focus on comparing different DL-based approaches for BP estimation. However, it is worth mentioning that direct comparisons between these methodologies based on the obtained results may not be entirely fair due to variations in the databases used, evaluation metrics employed, and preprocessing procedures applied. Nevertheless, such comparisons can be valuable in tracking the technical advancements in this field.

One notable study by González et al. [٣] introduced a benchmark that encompasses a wide range of datasets with diverse characteristics, allowing for more general conclusions to be drawn. This benchmark framework includes both handcrafted and automatically extracted features, with a tailored validation scheme and evaluation metrics for accurate comparisons of data-driven machine learning (ML) models. The authors demonstrated the effectiveness of their benchmark by comparing ١١ ML-based approaches and achieving a mean absolute error (MAE) of ١٦,٥٩ mmHg, and ٨,٣٠ mmHg for systolic and diastolic BP (SBP & DBP) using a ResNet architecture as the best result for the UCI database.

Another noteworthy work by Ibtehaz et al. presented PPG٢ABP, a two-stage cascaded DL method for estimating continuous arterial blood pressure (ABP) waveforms from input PPG signals [١٤]. They achieved an MAE of ٤,٦٠٤ mmHg for the UCI database, and it is worth mentioning that their approach obtained grade A ratings in the BHS standard for both DBP and mean arterial pressure (MAP), satisfying the AAMI standard.

Slapnič̆ar et al. employed PPG signals, along with their first and second derivatives, as inputs to a deep spectro-temporal neural network with residual connections [١٥]. Their proposed network, when personalized for each individual, effectively modeled the relationship between PPG and BP. For a subset of UCI data consisting of ٥١٠ subjects, they achieved an MAE of ٩,٤٣ mmHg for SBP and ٦,٨٨ mmHg for DBP.

Harfiya et al. introduced an LSTM-based autoencoder for translating raw PPG signals, along with their derivations, into ABP signals and extracting SBP and DBP values [١٣]. They achieved an MAE of ٤,٠٥ mmHg and ٢,٤١ mmHg for SBP and DBP, respectively, for a dataset comprising ٥٢٨٩ subjects. However, it is not explicitly mentioned whether they analyzed their framework in a personalized setting or not.

Although BP estimation from PPG signals holds promise, several challenges need to be addressed before it becomes clinically applicable. First, the accuracy of PPG-based BP estimation may be affected by undesired factors such as movement artifacts, ambient light interference, and changes in peripheral vascular

resistance. Second, individual calibration, which requires a reference BP measurement, is often necessary, limiting the convenience of the method. Finally, to date, the majority of research studies have been conducted on a small scale, highlighting the need for large-scale validation studies.

In this work, we propose and evaluate a variant of U-Net architecture called deep supervised multi-residual U-Net (DSMR-UNet) for direct BP estimation from raw PPG waveforms in a calibration-free setting. The contribution of this study includes:

١. Our approach utilizes a unimodal system consisting of a U-Net architecture, serving as a signal-to-signal translator. In contrast to estimating discrete values such as SBP and DBP, our model has the ability to estimate the complete waveshape of the ABP, which enhances the understanding of cardiovascular dynamics and can be particularly valuable in the healthcare domain.
٢. The proposed model exhibits exceptional learning capabilities for estimating the ABP signal. Unlike traditional methods that rely on hand-crafted PPG features, our model takes raw PPG signals as input. This eliminates the need for laborious feature engineering, as the model can learn directly from the raw data.
٣. Our method outperforms the majority of the studies reported in the literature, particularly when applied to large datasets.
٤. To assess the generalization performance of our model, we conducted validation on a separate test dataset collected by our team. The results obtained from this independent evaluation were highly encouraging, further confirming the promising performance of our model.

The rest of the paper is organized as follows: Section ٢ provides a comprehensive overview of the methodology employed in this study, which includes a detailed description of the datasets used, the various steps of data preprocessing, and finally the proposed U-Net pipeline. In section ٣, the experimental setup and evaluation metrics are outlined. Section ٤ presents the results obtained from the experiments, accompanied by interactive visualizations that enhance the understanding and interpretation of the outcomes. Finally, the paper concludes with Section ٥, which summarizes the main findings and contributions of the study and offers potential avenues for future research.

٢ Methodology

In this section, the datasets used in this study and the proposed methodology have been described in details.

٢,١ Databases

In this research, the Physionet's Multi-parameter Intelligent Monitoring in Intensive Care (MIMIC II) data, from the UCI Machine Learning Repository [١٦], termed as "UCI dataset," has been utilized. This dataset contains ١٢,٠٠٠ instances of simultaneous ECG, PPG, and ABP signals recorded from ٩٤٢ patients with a sampling rate of ١٢٥ Hz. SBP and DBP as target values were calculated from ABP waveforms. The statistical information on SBP and DBP values in the database is shown in Table ١.

In addition to the benchmark database, another native database named PPG_BP is collected, in order to examine the generalization capability of the methods. Data recording was performed using a fingertip pulse oximeter from Parsian Medical Company (ABADIS) equipped with a cuff-based BP monitoring device, which recorded the systolic/diastolic pressure at ٥-minute intervals during the test. To ensure the accuracy and reliability of the recorded values, an additional OMRON ٧٥٠it blood pressure monitor was employed

for cross-verification. The age range of the participants was ٢٠ to ٧٠ years. Participants were instructed not to place their feet on top of each other during the recording and to lean their backs against the chair they were sitting on while placing their hands on the table in a way that their arms were aligned with the heart. They were also instructed to remain motionless and maintain their composure during the recording. Subsequently, the BP of the right arm was measured, followed by a ٣٠-second interval, and then the BP of the left arm was measured. Immediately after the BP measurement, the recording of the PPG signal began. Indeed, after connecting the sensor to the participant's finger, a ٥-minute signal was recorded without any movement. Then, to create motion artifacts, they were asked to freely move the finger connected to the sensor (right hand), move their leg, take deep breaths, and continue recordings for approximately ٥ more minutes. After recording the PPG data, the BP of the right and left arms was measured again, and finally, the average recorded BP for each subject was considered as the ground truth. This dataset includes ٢٧٤ samples of systolic and diastolic BP information, as well as PPG signals, for ٢٧٠ individuals. The statistical information about the data is presented in Table ١.

Regarding our collected data, it should be emphasized that informed consent was obtained from each participant prior to the experiment, and the study protocol received approval from the "*Research Ethics Committees of Tarbiat Modares University (Approval ID: IR.MODARES.REC.1401.132)".*

Table 1: Overview of the datasets used in this study. Statistical information (minimum, maximum, average, and standard deviation) of SBP, DBP and MAP values in both UCI and PPG-BP data is presented.

Database	Parameters	Min(mmHg)	Max(mmHg)	Mean(mmHg)	STD(mmHg)
UCI	SBP	٧١,٨١	١٩٩,٩٨	١٤١,٠٣	٢٥,٦٤
	DBP	٥٠	١٤٨,٢٤	٥٧,٨٠	٩,٣١
	MAP	٥٧,٣٧	١٦٠,٥٦	٨٥,٥٤	١١,٩٥
PPG-BP data	SBP	٨٧	٢٠٣	١٢١,٩٩	١٧,٤٢
	DBP	٤٥	١٢٢	٧٦,٥٣	١٠,٥٦
	MAP	٧٦,٦٦	١٧٢,٦٦	١٠٦,٨٤	١٤,٢٢

٢,٢ Overview of the Proposed Methodology

Figure ١ provides an overview of the proposed framework. The PPG and ABP data from the UCI dataset are subjected to a preprocessing step before being used to train the model. When the regression model is designed and optimized based on UCI data, we test the model for our collected data (PPG-BP data). Similarly, the PPG signal in the PPG-BP data undergoes the same preprocessing step before being evaluated by the model. The model generates a continuous ABP signal as its output, from which we can extract the systolic and diastolic BP values. In the following sections, we will delve into the specific details of each step, providing a comprehensive explanation.

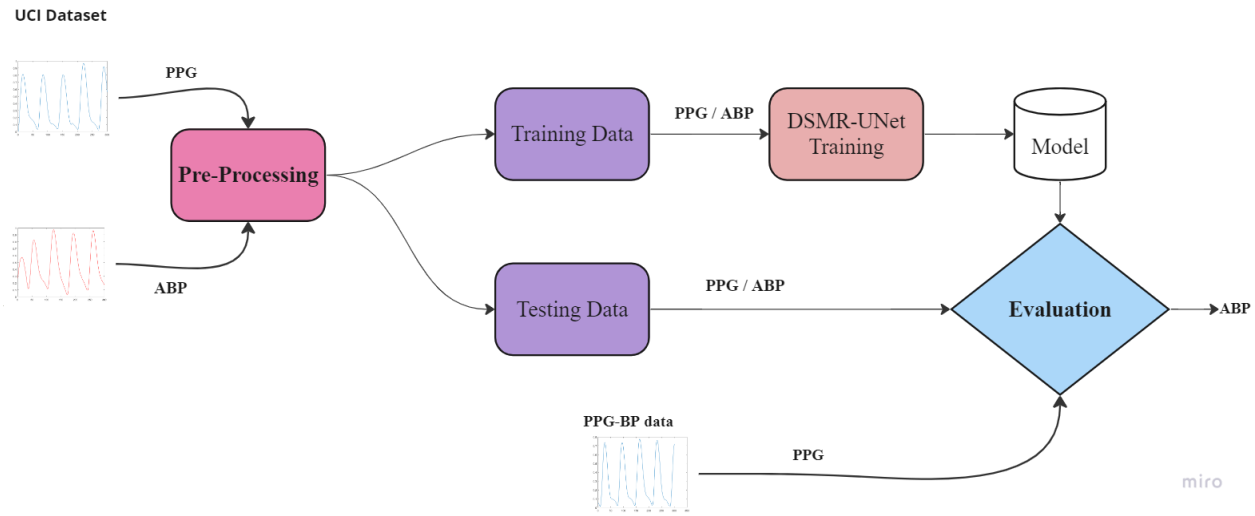

Figure 1: Overview of the proposed methodology.

٢,٣ Preprocessing

Data preprocessing is one of the critical steps for ML model training as it removes signal artifacts to improve the prediction performance, decrease the processing time and computational cost required to train the model, reduce the probability of model overfitting, and improve the interpretability of the model. In the current study, this process has been established as a widely adopted and common procedure used in the related literature [١٠].

In order to reduce the adverse effects of noise and artifacts present in the raw signals, a wavelet-based noise removal block has been implemented to enhance the signal quality [١٧]. Afterward, both PPG and ABP signals were segmented into ١٠٢٤ samples while maintaining the original sampling rate of ١٢٥ Hz. To address the issue of significant baseline drift observed in numerous cases, baseline wandering was eliminated prior to normalization. Additionally, following previous research [١٨], all samples outside the predefined systolic and diastolic ranges were removed to discard the outliers (the accepted range was considered ٥٠–١٢٠ for DBP, ٧٥–١٩٠ for SBP, and ٢٠–١٢٠ for BP difference).

Figure ٢. depicts an overview of the preprocessing pipeline.

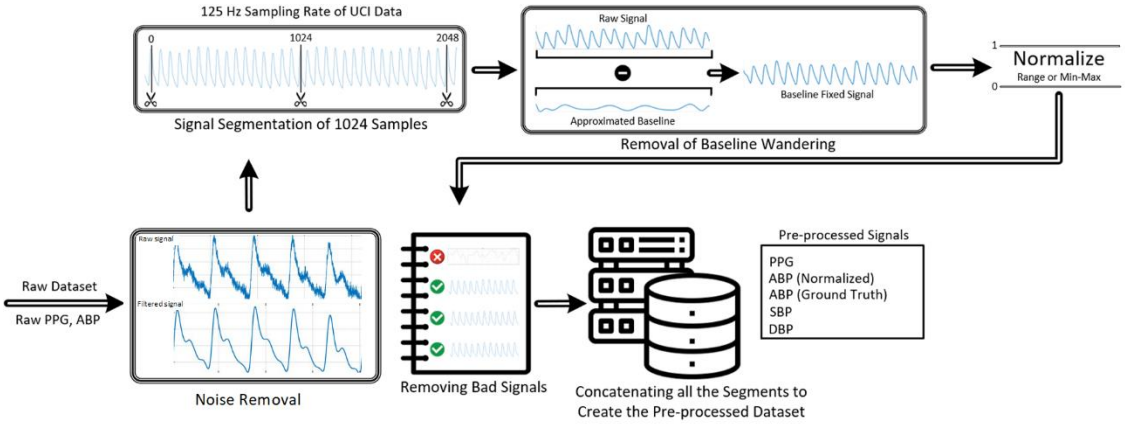

Figure 2: Raw signal preprocessing pipeline(adapted from [٣])

٢,٤ DSMR-UNet Architecture

In this research, a signal-to-signal regression model based on a variant of the U-Net architecture has been proposed. It should be noted that the 'signal-to-signal' model includes models that estimate ABP signals from PPG signals.

The U-Net architecture has gained significant popularity as the leading neural network model in the domain of medical imaging, especially semantic segmentation tasks. Over time, several modifications have been proposed to enhance its performance and adapt it to evolving needs [١٩]. Taking inspiration from the profound insights gained from recent advancements in deep computer vision, we have made further modifications to the U-Net architecture. By incorporating the multi-residual blocks and deep supervision into the design, we proposed the DSMR-UNet framework with the aim of achieving improvement and refinement in our regression task. The key components of the proposed architecture are as follows:

(a) U-Net architecture: The U-Net architecture consists of an encoder-decoder structure. The encoder part captures context and learns high-level features from the input signal, while the decoder part performs up-sampling to generate a segmentation map with the same resolution as the input image. The U-Net architecture has skip connections that allow information flow from the encoder to the decoder, preserving more spatial details.

(b) Multi-residual blocks: The multi-residual blocks are a variation of the traditional residual blocks used in neural networks. These blocks consist of multiple convolutional layers with residual connections. The residual connections enable the network to learn residual functions, making it easier to optimize the training process.

(c) Deep supervision: Deep supervision involves introducing intermediate supervision signals in the network, allowing for the extraction of features at different depths. In the deep supervised multi-residual U-Net, intermediate supervision is incorporated by adding auxiliary regressors at different levels of the decoder. These regressors help guide the training process and provide additional gradients for better learning.

(d) Supervised learning: The model is trained in a supervised manner. It requires a dataset with labeled examples, where each input image is paired with its corresponding continuous-valued output signals. The network learns to map input signals to their respective output signals by minimizing a suitable loss function, such as cross-entropy or Dice loss.

By leveraging the DSMR UNet architecture, the network can effectively learn the underlying patterns and relationships in the input signals, allowing it to regress and estimate continuous-valued output signals accurately. This approach has applications in various domains such as speech processing, audio synthesis, and time series forecasting, where the goal is to predict the continuous signals.

Figure ٣ depicts our proposed model.

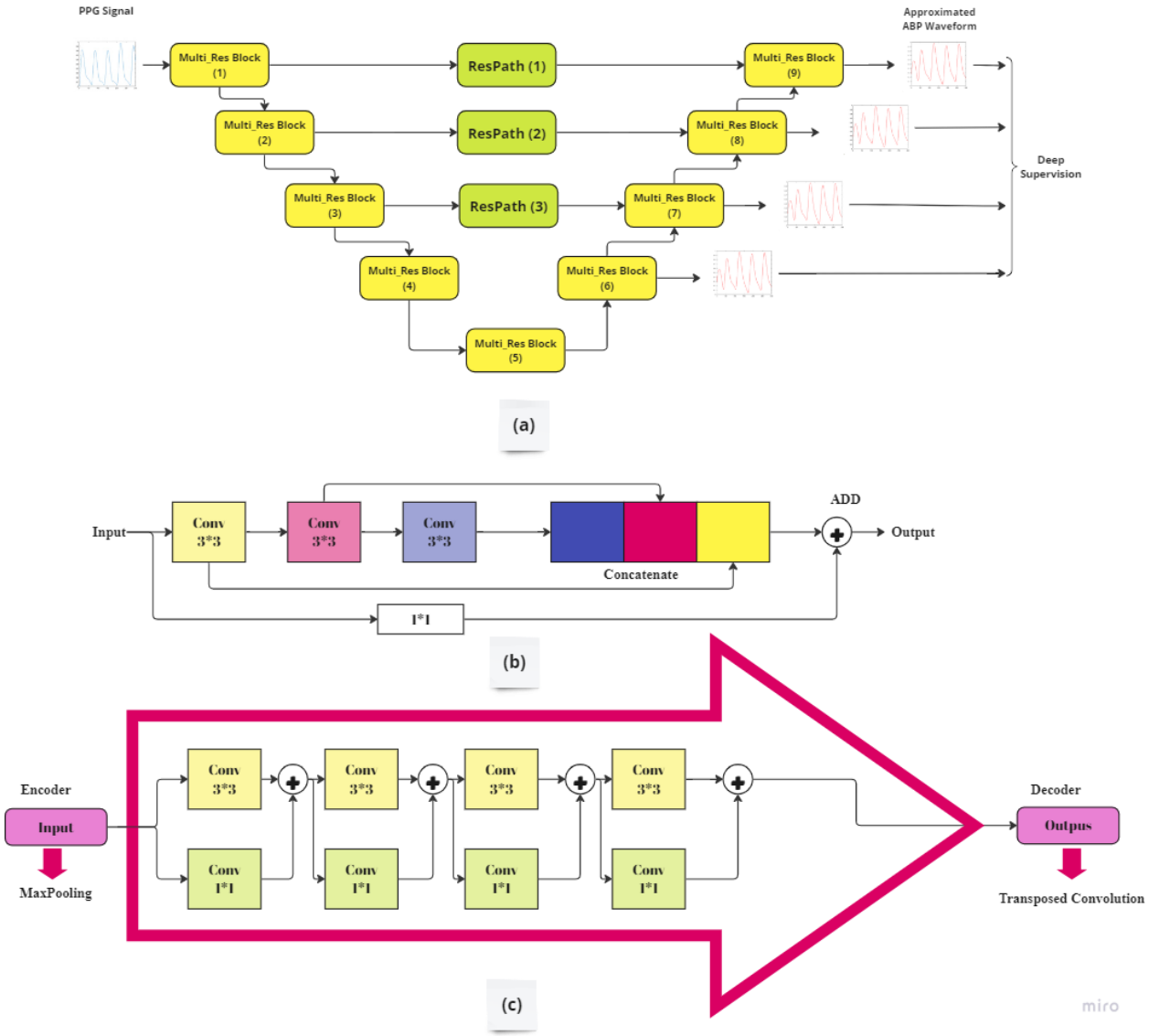

Figure 3: The architecture of the proposed regression model (a) DSMR-UNet pipeline consisting of multi-residual blocks and residual paths; (b) the architecture of a multi-residual block; (c) inside of a residual path.

۳ Evaluation Metrics and Experimental Setting

Evaluating regression models involves assessing how well the model fits the data and how accurate its predictions are. There are several common evaluation metrics used for regression models: mean absolute error (MAE), standard deviation of absolute error (STD), mean square error (MSE) and $R^{۲}$-score. The definition of these metrics is given in Eq. (۱)-Eq. (٤).

$MAE = \frac{\sum_{i=1}^{n} \lvert y_i - y_i' \rvert}{n}$	Eq. (۱)
$Std = \sqrt{\frac{\sum_{i=۱}^{n} (y_i - y_i')^{۲}}{n}}$	Eq. (۲)

$MSE = \frac{\sum_{i=1}^{n}(y_i - y_i')^2}{n}$	Eq. (3)
$R^2 - score = 1 - \frac{\sum_{i=1}^{n}(y_i - y_i')^2}{\sum_{i=1}^{n}(y_i - \bar{y})^2}$	Eq. (4)

where y_i and y_i' represent the ground truth and estimated output value for n samples. $\bar{y}$ denotes the average value for ground truths.

These metrics are used to evaluate the proposed method. Additionally, we conducted a comparison of our findings with the guidelines provided by the BHS (British Hypertension Society) and the AMMI (Association for the Advancement of Medical Instrumentation). The BHS guideline classifies the accuracy of BP measurement into three categories, each corresponding to different estimation ranges. On the other hand, the AMMI standard focuses on evaluating the error and standard deviation.

Moreover, we utilized Bland-Altman plots to visually represent the agreement between the model-predicted and true values [20] of blood pressure. In these plots, the X-axis represents the mean value, while the Y-axis depicts the differences between the estimated and true values, along with 95٪ confidence intervals.

4 Results

the experiments have been performed using Pytorch3,11 running on a desktop workstation equipped with an NVIDIA 24 GB GeForce RTX 3090 GPU card.

It is worth mentioning that the dataset was divided into three sets: 70٪ for the training dataset, 15٪ for the validation dataset, and 15٪ for the testing dataset. In this data split method, no information leakage occurred between the training and testing data to ensure that the method was executed without individual calibration.

4,1 Experiment1: Train and test on UCI data

4,1,1 Results of ABP Estimation

Since the primary objective of this research is to provide continuous blood pressure estimation from the input PPG signal, in the initial experiments conducted, we present here the accuracy of ABP signal estimation both qualitatively and quantitatively. Figure 4 displays one of the input PPG waveforms, and the generated ABP output signal from the proposed network. As shown in this figure, the estimated blood pressure signal from the DSMR-UNet has been able to produce a good approximation of the reference ABP signal. However, lower accuracy is observed in estimating the maximum BP, namely systolic pressure (SBP). In terms of quantitative evaluation, the MAE of the continuous BP signal is 4,74 mmHg, indicating the relative success of the approach employed in this research.

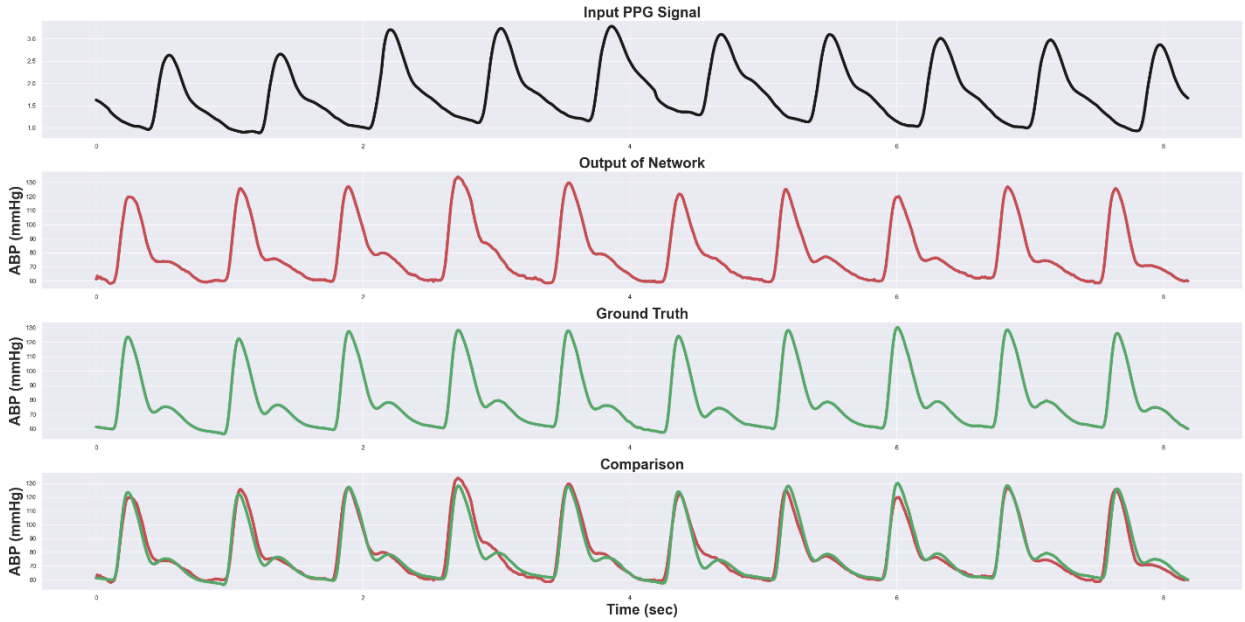

Figure 4: The display of network outputs at each stage in the proposed DSMR-UNet architecture. The plots, from top to bottom, represent the input PPG signal, the network's output in estimating ABP, the reference ABP signal, and the comparison between the network's output and the reference signal.

٤,١,٢ Results of BP Parameters Estimation

Given that the output of the designed network is the continuous ABP signal, the model evaluation should compute a specific value for the systolic, diastolic, and mean blood pressure for each signal segment. to achieve this goal, the median of the maximum and minimum values of the ABP signal in each segment is calculated as the systolic and diastolic values, respectively. Mean arterial pressure (MAP) is calculated by Eq. (٥).

$$MAP = \frac{(SBP + ٢DBP)}{٣} \qquad \text{Eq. (٥)}$$

Table ٢ presents an evaluation of the proposed framework for SBP, DBP and MAP values in terms of estimated errors and $R^{٢}$-score. As reported in this table, the error in estimating systolic pressure is higher than the error in estimating diastolic and average pressure error. The standard deviation of SBP estimation is also higher than DBP and MAP. The best $R^{٢}$-score belongs to DBP estimation which means that our regression model explains ٩٤٪ of the variation in our diastolic variable.

Table 2: Performance evaluation for UCI data in terms of estimation error: MAE, STD, MSE, and R^2-score.

	MAE	STD	MSE	$R^{٢}$-score
SBP	٤.٣٤	٥.٦٣	٥٠.٦٣	٠.٥٥
DBP	٣.٣٢	٤.٦٣	٣٢.٥١	٠.٩٤
MAP	٢.٤٩	٣.١٢	١٥.٩٣	٠.٩٢

٤,١,٣ Results Evaluation Based on International Standards

The performance of proposed method based on BHS standard is presented in Table ٣. The results demonstrate that using the developed pipeline, we have achieved grade A for SBP, DBP, and MAP. The histogram of absolute error in the estimation of blood pressure parameters is depicted in Figure ٥. As expected, for the DBP and MAP, the absolute error for almost no predictions is higher than ١٥ mmHg, but for the SBP prediction, there are a few samples with errors higher than ١٥ mmHg.

Furthermore, we assessed the performance of the model using the AMMI standard, as presented in Table ٤. The results indicate that our predictions meet the criteria set by AMMI.

To visualize the error measurements for SBP, DBP, and MAP predictions, we plotted them in Figure ٦. The distribution of errors follows a normal distribution, which aligns with the Central Limit Theorem. Notably, the SBP predictions exhibit a wider distribution compared to the DBP and MAP predictions, suggesting a higher level of deviation and lower accuracy in the SBP predictions, while still remaining in standard range.

Table 3: Model evaluation for UCI data based on BHS standard. All predicted BP values for UCI data meet grade A.

Cumulative Error Percentage				
		<=٥ mmHg	<=١٠mmHg	<=١٥mmHg
Our Results	SBP (A)	٧٢,٩٪	٩٠,٧٪	٩٥,٣٪
	DBP (A)	٨٣,٩٪	٩٥,٠٪	٩٧,٧٪
	MAP (A)	٨٨,٢٪	٩٧,٠٪	٩٨,٩٪
BHS Metric	Grade A	٦٠٪	٨٥٪	٩٥٪
	Grade B	٥٠٪	٧٥٪	٩٠٪
	Grade C	٤٠٪	٦٥٪	٨٥٪

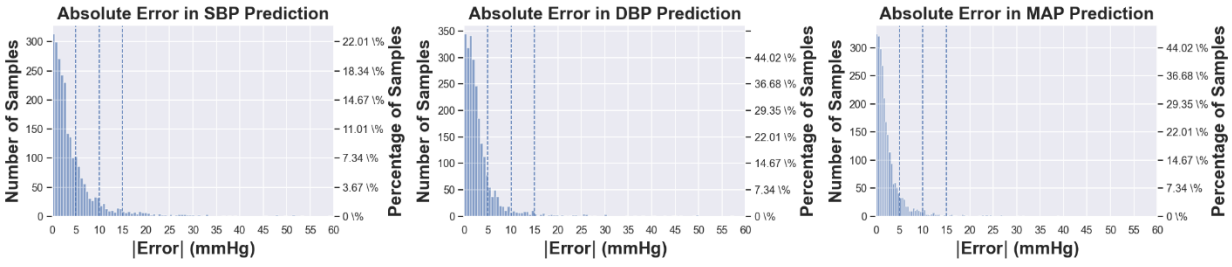

Figure 5: Histogram of absolute error in estimation of SBP, DBP, and MAP from left to right.

Table 4: Model evaluation for UCI data based on AAMI standard. All predicted BP values for UCI data meet the criteria.

		ME	STD
Our Results	SBP	٠,٥٣	٧,٠٩
	DBP	-٠,٠٧	٥,٧٠
	MAP	-٠,٥٥	٣,٩٥
AAMI Metric		<=٥	<=٨

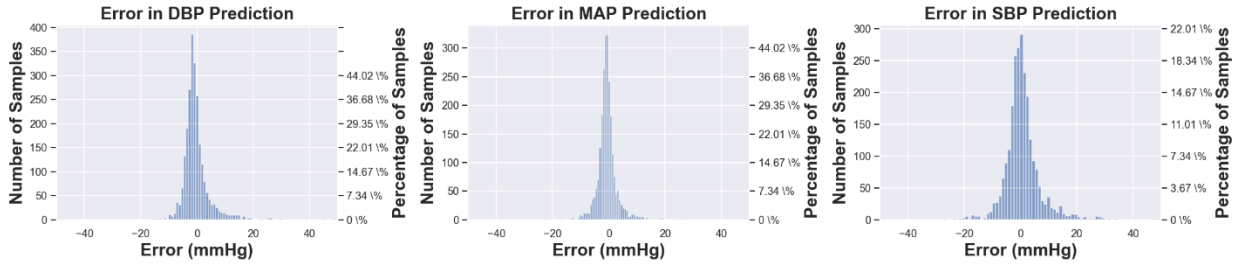

Figure 6: Error distribution for DBP, MAP, and SBP from left to right.

٤,١,٤ Statistical Analysis

Figure ٧ illustrates the response plots for the regression outcomes of DBP, MAP, and SBP, showcasing a clear and significant correlation between the predicted and target values. The Pearson correlation coefficients for DBP, MAP, and SBP predictions are ٠,٨٥, ٠,٩٦, and ٠,٩١ respectively. These coefficients indicate a strong degree of correlation between the predicted variables and the ground truths in all cases.

Figure ٨ shows the Bland-Altman plots as an agreement indicator for BP parameters provided by the measurement and estimation. The dashed lines represent the ٩٥٪ limits of agreement, which correspond to the ranges [-١١,٢٤:١١,١٠], [-٨,٣٠:٧,١٩], and [-١٣,٣٦:١٤,٤٣] mmHg, for DBP, MAP, and SBP respectively. Since in all three cases, more than ٠,٩٥ of data is between the determined limits, we could conclude the agreement between our estimated BP parameters with the measured ones. Although the errors may seem large when observing the plots in Figure ٨, it is evident that the majority of the error terms fall within a range of ٥ mmHg.

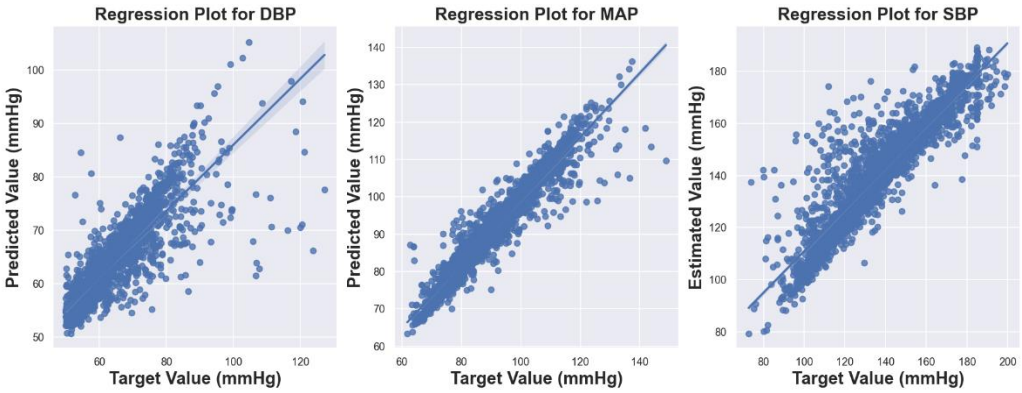

Figure 7: Regression plot for DBP, MAP, and SBP predictions from left to right respectively.

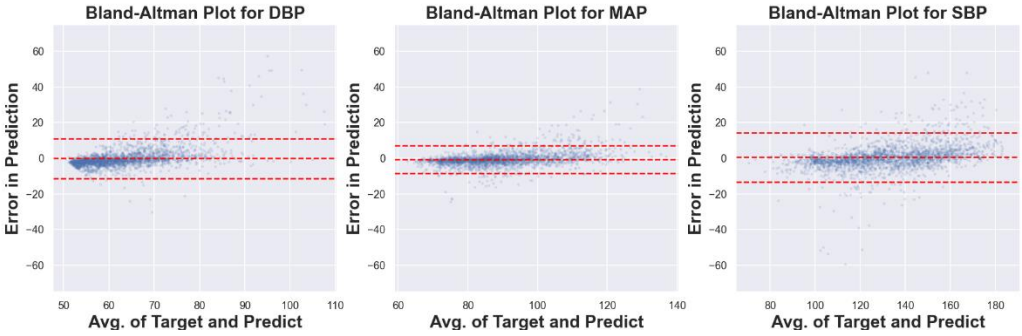

Figure 8: Bland-Altman plot for DBP, MAP, and SBP from left to right. The dashed lines represent the 95% limits of agreement.

٤,١,٥ Results Evaluation Based on Blood Pressure Categories

At the end of this section, for further examination of the results obtained from the proposed model, we performed the classification of DBP and SBP into three groups: normal, prehypertension, and hypertension, which are indicated in Table ٥ as the corresponding BP ranges. The results of this evaluation are presented in Figure ٩. In the estimation of DBP, the model achieved good accuracy (١٠٠٪) in classifying the normal BP group, while the accuracy of classifying the prehypertension and hypertension groups is relatively low (٣٨٪ versus ٢٢٪). However, in the estimation of SBP, the best classification accuracy was observed for the hypertension group (٩٢٪), followed by the normal and prehypertension groups (٨٧٪ and ٨٦٪, respectively). While our previous findings indicated that our model exhibited higher errors in estimating SBP compared to DBP and MAP, it successfully classified high-risk hypertension cases. This implies that, despite the challenges in SBP estimation, our model may be helpful in identifying cases of elevated hypertension risk. Furthermore, we present the classification performance of our test data in terms of macro average accuracy, precision, recall, and F١-score in Table ٦. The results indicate that the accuracy achieved for DBP is higher than that of SBP. However, when considering other evaluation metrics, the classification of SBP demonstrates better results.

Table 5: The range of systolic and diastolic pressure in three classes: normal, prehypertension, and hypertension.

BP categories	DBP (mmHg)	SBP (mmHg)
Normal	٦٠-٨٠	٨٠-١٢٠
Prehypertension	٨٠-٩٠	١٢٠-١٤٠
Hypertension	>٩٠	>١٤٠

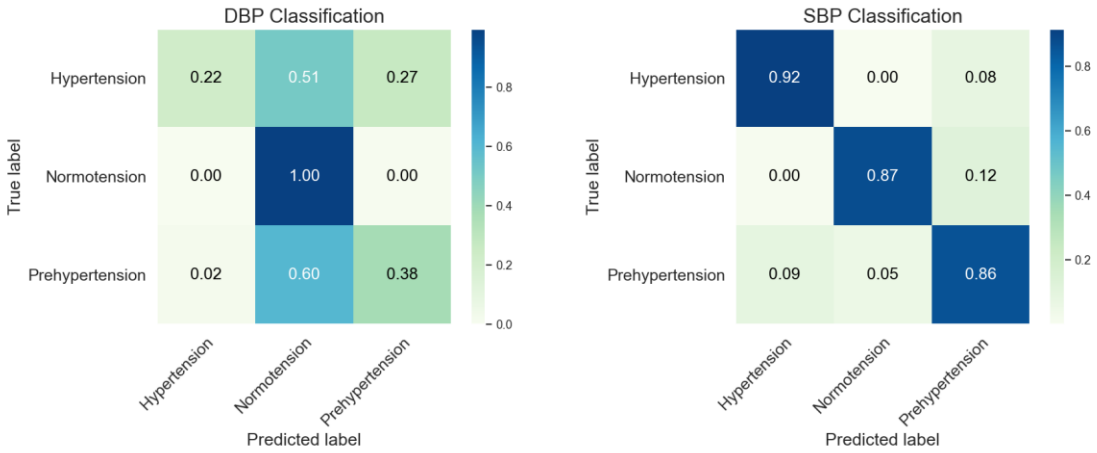

Figure 9: Classification of diastolic and systolic BP into three classes: normal blood pressure, prehypertension, and high blood pressure using the proposed DSMR_UNet architecture.

Table 6: Classification performance of diastolic and systolic BP into three categories (normal, prehypertension, and high blood pressure) in terms of macro average accuracy, precision, recall, and F1-score.

BP values	Accuracy	Precision	Recall	F١-score
SBP	٨٨,٥٦	٨٨,٣٢	٨٨,٢٦	٨٨,١٥
DBP	٩٥,١٤	٨١,٩٣	٥٣,٣٥	٦٠,٤٣

٤,٢ Experiments٢: Train on UCI data, test on PPG-BP data

In this experiment, the proposed model was trained on the entire pre-processed UCI dataset and subsequently tested on the complete PPG-BP dataset (which was also pre-processed in a similar manner). The primary objective was to demonstrate the efficacy of the regression model trained on a large dataset when applied to an external dataset.

A notable point in this section is that we do not have access to the ABP signal for the recorded data in PPG_BP dataset. We only have access to the systolic and diastolic BP values, which were measured multiple times during the experiment using two calibrated BP devices. Therefore, the reference BP for this

dataset is considered as the average of all the measured BPs for systolic and diastolic readings for each individual.

Table ٧ showcases an assessment of the proposed framework based on estimated errors and R^2-score. As indicated in the table, the error in estimating systolic pressure exceeds that of diastolic BP, along with a higher STD of errors. Additionally, both measurements exhibit a negative R^2-score, indicating suboptimal predictive performance, compared to previous results presented in Table ٢.

According to the BHS standard as shown in Table ٨, our proposed model for the PPG-BP data will not have clinical applicability. However, in the next section, further discussion of these findings and effective strategies to enhance the results will be suggested.

Table 7: Performance evaluation for PPG-BP data in terms of estimation error: MAE, STD, MSE, and R^2-score.

	MAE	STD	MSE	R^2-score
SBP	١٦.٣٣	١٢.٣٢	٤٣٨.٨٩	-٦.٥٧
DBP	٧.٤٥	٦.٤٤	٩٨.٩٤	-٥.٣٥

Table 8: Model evaluation for PPG-BP data based on BHS standard.

Cumulative Error Percentage				
		<=٥ mmHg	<=١٠mmHg	<=١٥mmHg
Our Results	SBP	١٧,٣٦٪	٣٠,٥٢٪	٤٥,٧٨٪
	DBP	٣٦,٨٤٪	٦٥,٧٩٪	٨٤,٧٣٪

٤,٣ Comparison to other works

Table ٩ presents a comparison of the results obtained from our proposed method with previous studies reported on a given dataset. Due to variations in the number of data used in previous research and differences in preprocessing methods for PPG signals and evaluation techniques, a direct comparison of the processing methods would not be fair. However, it is possible to provide a summary of the general approaches applied in various studies and their relative success in estimating BP from PPG signals as input to the model. As observed in this table, individual calibration-based studies, where a portion of an individual's data is used to train the regression model, show significant improvements in results. In fact, many studies have emphasized the impact of individual calibration on improving the results [١٣]. However, due to limitations in using such techniques in clinical applications, many researchers have attempted to increase the accuracy of blood pressure parameter estimation without relying on individual calibration. As

seen in Table ٦, the results of this study, considering the use of a large volume of data and the absence of individual calibration techniques, have achieved desirable outcomes compared to the state of the art.

Table 9: Comparison with other works. A summary of important information from previous research on the MIMIC database is provided (NA denotes the unavailability of information).

Work	**No. Subjects**	**Calibration**	**Error (MAE)**		**BHS standard**	
			SBP	DBP	SBP	DBP
[٢١]	١٠٥ records, ٨٣٨٠ samples	NA	١٧,٠٨	١٠,٧٧	NA	NA
[٢٢]	١٣٢٣ records	No	٣,٩٧	٢,٤٣	C	A
[٢٣]	١٩١٢ subjects	Yes	٥,٣٢	٣,٣٨	B	A
[٢٤]	١٥٥٧ records	NA	٣,٩٧	٢,٣٠	A	A
[٢٥]	٩٤٢ subjects	No	٨,٢٢	٤,١٧	C	A
[٢٦]	١١٥٤٦ samples	No	٥,٥٩	٣,٣٦	B	A
[٢٧]	١٢١٦ records	Yes	٣,٧٠	٢,٨١	A	A
[٢٨]	٢٠٠ records	NA	٣,٠٥	١,٥٨	A	A
[٢٩]	٩٠٠٠ records	NA	٣,٢١	٢,٢٣	A	A
[٣٠]	١٦٢٠ records, ٢٧٧٠٥٠ samples	Yes	٧,١٥	٥,٥٧	NA	NA
[٣١]	٣١٨٣ subjects, ٩٥٤٩ samples	NA	٣,٩٦	٢,٣٩	A	A
[٣٢]	٥٢٨٩ records, ٢٥٠٠٠٠ samples	NA	٤,٠٥	٢,٤١	A	A
[٣٣]	Unknown records, ٥٠١٦٥ samples	Yes	٥,٤٢٤	٣,١٤٤	C	A
Our Work	٩٠٠٠٠ records	No	٤,٣٤	٣,٣٢	A	A

٥ Discussion and Conclusion

BP is a vital health indicator that requires continuous measurement and monitoring for the diagnosis and control of cardiovascular diseases. Traditional methods of BP measurement, like BP cuffs, require complex and intrusive equipment. Therefore, the use of non-invasive and indirect methods for estimating BP has gained attention. The PPG signal, as one of the simple and non-invasive methods that measures changes in blood volume can provide insights into an individual's BP. In this study, we investigated the use of PPG signals for continuous BP estimation using deep neural networks. Estimating the waveform of the BP signal has precedence over estimating the overall values of systolic and diastolic pressures. In general, estimating the waveform of the BP provides more accurate information about cardiovascular function and its changes over time, which can be useful in disease diagnosis and BP monitoring.

In this research, a DL model called DSMR-UNet was employed for continuous BP estimation. The use of deep supervision usually leads to increased accuracy and performance of the models. This is because having intermediate outputs and computing losses for them guides the learning process better, and the hidden layers of the model also could be trained independently. This can result in more optimal utilization of information within the data and the extraction of more useful features. Additionally, auxiliary losses from lower layers to upper layers with reduced weights are calculated, allowing the model to learn in a balanced and

continuous manner throughout the training structure. This typically leads to a significant increase in accuracy and a reduction in overall model errors. However, the success of deep supervision depends on the features and architecture of the model, and in some cases, its impact may be less significant or not yield noticeable improvements. In addition to deep supervision, we incorporated the multi-residual blocks into our proposed model. Indeed, the use of multi-residual blocks in U-Net helps in creating a more powerful and effective model by addressing the challenges posed by deeper networks: addressing vanishing gradients, facilitating information flow, and promoting feature reuse [١٩].

The proposed model was evaluated on the UCI dataset, achieving MAE of ٤,٣٢, ٣,٣٤, and ٢,٤٩, and STD of ٥,٦٣, ٤,٦٣, and ٣,١٢, respectively, for systolic, diastolic, and mean BP. As mentioned in the results section, according to the BHS standard, all BP parameters achieved an A grade. This means that the proposed model has good accuracy for estimating the BP parameters and is recommended for clinical applications.

In the analysis of the native recorded data from the PPG-BP dataset, due to the limited amount of data, it was not possible to train a deep neural network. Therefore, we used the best-trained model on the UCI dataset and kept the network weights constant while performing the testing phase on the PPG-BP data. As mentioned earlier, we did not have access to the ABP signal for this database, and we only had access to the values of systolic and diastolic BP, which were measured multiple times during the experiment with two cuff-based BP devices. Therefore, the reference BP for this data was the average of all the measured BPs for systolic and diastolic values for each individual.

Ultimately, on the native data, we achieved MAE of ١٦,٣٣ and ٧,٤٥, and STD of ١٢,٣٢ and ٦,٤٤, respectively, for SBP and DBP. Although, according to the BHS and AMMI-defined standards, these results did not reach an acceptable accuracy for clinical use, they pave the way for future research to make this work more practical. In the conducted investigations, one of the reasons for not achieving the desirable results that we obtained in the UCI database was the unavailability of reliable reference BP for the recorded data. In fact, we used two different BP monitors to collect the data, and we recorded from the left and right sides of individuals at various time intervals. The goal was to remove the data if the difference in BPs for an individual exceeded a certain threshold. However, ultimately, due to the large number of samples that had to be removed, we had to abandon this decision. In this project, we used the average pressure for each individual, but to solve this problem, in future studies, more samples can be recorded so that if there is a significant difference between the recorded pressures from the left and right sides or different BP monitors for a sample, it can be eliminated.

Another reason for the not-so-desirable results in the processing of PPG-BP data is the presence of highly disruptive motion noise in the PPG signal of this data. In the preprocessing stage, we used common noise removal methods, including inappropriate frequency band filtering. However, due to the frequency band interference of motion noise with the PPG signal, more complex methods should be used for this purpose. One of the suggested methods to solve this problem is the use of AI techniques [٥٦].

To conclude, PPG signal-based BP estimation provides a promising method for non-invasive, continuous BP monitoring. However, more research is needed to improve the accuracy, robustness, and convenience of the method. As wearable technology continues to advance, we can expect improved techniques for PPG-based BP estimation, leading to better hypertension management and prevention of cardiovascular diseases.

Declarations

Human ethics and consent to participate

The study protocol received ethics approval from the "*Research Ethics Committees of Tarbiat Modares University (Approval ID: IR.MODARES.REC.1401.132)"*. All participants were provided with comprehensive information regarding the voluntary nature of their participation, with an explicit assurance of no potential risks. Furthermore, the confidentiality of their identities was guaranteed.

Consent for publication

Despite ensuring that participants' data remained entirely unidentifiable and no individual details were included in the manuscript, consent from each participant was obtained for the publication.

Availability of data and materials

Availability of data and materials: The UCI dataset is available from https://drive.google.com/drive/folders/١n٢٤ahZCxAAdkkmCfVrQeZXsSl٤w٠P٦Jg, and PPG-BP dataset as well as the source code will be available upon reasonable request (contact to corresponding author: *S. Sh., E-mail: s.shojaie@irost.ir*).

Competing interests

The authors declare there is no competing of interest.

Funding

This work was part of a project (ID: ١٠١٠٨٠١٠٠١) supported by IROST.

Authors' contributions

S. Sh. and M. Kh. performed programming. S. Sh. and M. M wrote the manuscript draft. S. Sh. analyzed the experiment. S.S. and M. B. edited the manuscript, checked the data and supervised the project.

Acknowledgment

We would like to express our appreciation to "Parsian Medical" company for providing the pulse-oximeter device for the purpose of collecting PPG-BP dataset.

References

[١] X. Ding, B. P. Yan, Y. Zhang, J. Liu, N. Zhao, and H. K. Tsang, "Pulse Transit Time Based

Continuous Cuffless Blood Pressure Estimation : A New Extension and A Comprehensive Evaluation," *Sci. Rep.*, no. May, pp. ١–١١, ٢٠١٧, doi: ١٠,١٠٣٨/s٤١٥٩٨-٠١٧-١١٥٠٧-٣.

[٢] N. Maher, G. A. Elsheikh, W. R. Anis, and T. Emara, "Enhancement of blood pressure estimation method via machine learning," *Alexandria Eng. J.*, vol. ٦٠, no. ٦, pp. ٥٧٧٩–٥٧٩٦, ٢٠٢١, doi: ١٠,١٠١٦/j.aej.٢٠٢١,٠٤,٠٣٥.

[٣] S. González, W. Hsieh, and T. P. Chen, "A benchmark for machine- learning based non-invasive blood pressure estimation using photoplethysmogram," *Sci. Rep.*, pp. ١–١٦, ٢٠٢٣, doi: ١٠,١٠٣٨/s٤١٥٩٧-٠٢٣-٠٢٠٢٠-٦.

[٤] B. Engineering, C. Academy, and K. Road, "Optical blood pressure estimation with photoplethysmography and FFT-based neural networks," *Biomed. Opt. Express*, vol. ٧, no. ٨, pp. ٧١–٧٤, ٢٠١٦.

[٥] N. Hasanzadeh, M. M. Ahmadi, and H. Mohammadzade, "Blood Pressure Estimation Using Photoplethysmogram Signal and Its Morphological Features," *IEEE Sens. J.*, vol. ٢٠, no. ٨, pp. ٤٣٠٠–٤٣١٠, ٢٠٢٠.

[٦] V. Figini, S. Galici, D. Russo, I. Centonze, M. Visintin, and G. Pagana, "Improving Cuff-Less Continuous Blood Pressure Estimation with Linear Regression Analysis," *electronics*, vol. ١١, pp. ١–١٨, ٢٠٢٢.

[٧] M. Simjanoska, M. Gjoreski, M. Gams, and A. M. Bogdanova, "Non-invasive blood pressure estimation from ECG using machine learning techniques," *Sensors (Switzerland)*, vol. ١٨, no. ٤, pp. ١–٢٠, ٢٠١٨, doi: ١٠,٣٣٩٠/s١٨٠٤١١٦٠.

[٨] S. Haddad, A. Boukhayma, and A. Caizzone, "Continuous PPG-Based Blood Pressure Monitoring Using Multi-Linear Regression," pp. ١–٩, ٢٠٢٠.

[٩] H. Hashemzadeh, S. Shojaeilangari, and A. Allahverdi, "A combined microfluidic deep learning approach for lung cancer cell high throughput screening toward automatic cancer screening applications," *Sci. Rep.*, pp. ١–١٠, ٢٠٢١, doi: ١٠,١٠٣٨/s٤١٥٩٨-٠٢١-٨٩٣٥٢-٨.

[١٠] S. Mahmud *et al.*, "A Shallow U-Net Architecture for Reliably Predicting Blood Pressure (BP) from Photoplethysmogram (PPG) and Electrocardiogram (ECG) Signals," *sensors*, vol. ٢٢, ٢٠٢٢.

[١١] S. Yang, Y. Zhang, S. Y. Cho, R. Correia, and S. P. Morgan, "Non-invasive cuff-less blood pressure estimation using a hybrid deep learning model," *Opt. Quantum Electron.*, vol. ٥٣, no. ٢, pp. ١–٢٠, ٢٠٢١, doi: ١٠,١٠٠٧/s١١٠٨٢-٠٢٠-٠٢٦٦٧-٠.

[١٢] D. U. Jeong and K. M. Lim, "Combined deep CNN – LSTM network - based multitasking learning architecture for noninvasive continuous blood pressure estimation using difference in ECG - PPG features," *Sci. Rep.*, no. ٠١٢٣٤٥٦٧٨٩, pp. ١–٨, ٢٠٢١, doi: ١٠,١٠٣٨/s٤١٥٩٨-٠٢١-٩٢٩٩٧-٠.

[١٣] C. Blood, P. Estimation, and U. Exclusively, "Continuous Blood Pressure Estimation Using Exclusively Photopletysmography by LSTM-Based Signal-to-Signal Translation," ٢٠٢١.

[١٤] N. Ibtehaz *et al.*, "PPG٢ABP : Translating Photoplethysmogram (PPG) Signals to Arterial Blood Pressure (ABP) Waveforms," *bioengineering*, vol. ٩, ٢٠٢٢.

[١٥] G. Slapnicar, N. Mlakar, and M. Luštrek, "Blood Pressure Estimation from Photoplethysmogram Using a Spectro-Temporal Deep Neural Network," *sensors*, vol. ١٩, ٢٠١٩, doi: ١٠,٣٣٩٠/s١٩١٥٣٤٢٠.

[١٦] H. & S. Kachuee, M., Kiani, M. M., Mohammadzade, "Cuff-less blood pressure estimation data set," ٢٠١٥. https://archive.ics.uci.edu/ml/datasets/Cuff-Less+Blood+Pressure+Estimation.

[١٧] M. Kachuee, S. Member, M. M. Kiani, and S. Member, "Cuff-Less Blood Pressure Estimation Algorithms for Continuous Health-Care Monitoring," *IEEE Trans. bio-medical Eng.* ·, vol. ٦٤, no. ٤, ٢٠١٦, doi: ١٠,١١٠٩/TBME.٢٠١٦,٢٥٨٠٩٠٤.

[١٨] S. Mahmud *et al.*, "Biomedical Signal Processing and Control NABNet : A Nested Attention-guided BiConvLSTM network for a robust prediction of Blood Pressure components from reconstructed Arterial Blood Pressure waveforms using PPG and ECG signals," *Biomed. Signal Process. Control*, vol. ٧٩, no. P٢, p. ١٠٤٢٤٧, ٢٠٢٣, doi: ١٠,١٠١٦/j.bspc.٢٠٢٢,١٠٤٢٤٧.

[١٩] N. Ibtehaz and M. S. Rahman, "MultiResUNet : Rethinking the U-Net architecture for multimodal

biomedical image segmentation," *Neural Networks*, vol. ١٢١, pp. ٧٤–٨٧, ٢٠٢٠, doi: ١٠,١٠١٦/j.neunet.٢٠١٩,٠٨,٠٢٥.

[٢٠] U. Bland and D. Giavarina, "Understanding Bland Altman analysis," *Biochem. Medica*, vol. ٢٥, no. ٢, pp. ١٤١–١٥١, ٢٠١٥.

[٢١] S. N. B. S and A. Kandaswamy, "Sparse characterization of PPG based on K- SVD for beat-to-beat blood pressure prediction .," vol. ٢٩, no. ٤, pp. ٨٣٥–٨٤٣, ٢٠١٨.

[٢٢] G. Y. Mousavi SS, Firouzmand M, Charmi M, Hemmati M, Moghadam M, "Blood pressure estimation from appropriate and inappropriate PPG signals using a whole-based method," *Biomed Signal Process Control*, vol. ٤٧, pp. ١٩٦–٢٠٦, ٢٠١٩.

[٢٣] S. Baek, "End-to-End Blood Pressure Prediction via Fully Convolutional Networks," *IEEE Access*, vol. ٧, pp. ١٨٥٤٥٨–١٨٥٤٦٨, ٢٠١٩, doi: ١٠,١١٠٩/ACCESS.٢٠١٩,٢٩٦٠٨٤٤.

[٢٤] A. A. Panwar M, Gautam A, Biswas D, "PP-Net: a deep learning framework for PPG-based blood pressure and heart rate estimation," *IEEE Sens J*, vol. ٢٠, no. ١٧, pp. ١٠٠٠٠–١٠٠١١, ٢٠٢٠.

[٢٥] M. H. Hasanzadeh N, Ahmadi MM, "Blood pressure estimation using photoplethysmogram signal and its morphological features," *IEEE Sens J*, vol. ٢٠, no. ٨, pp. ٤٣٠٠–٤٣١٠, ٢٠١٩.

[٢٦] M. Rong and K. Li, "A multi-type features fusion neural network for blood pressure prediction based on photoplethysmography," *Biomed Signal Process Control*, vol. ٦٨, p. ١٠٢٧٧٢, ٢٠٢١.

[٢٧] Y. Qiu *et al.*, "blood pressure estimation based on composite neural network and graphics information," *Biomed. Signal Process. Control*, vol. ٧٠, no. July, p. ١٠٣٠٠١, ٢٠٢١, doi: ١٠,١٠١٦/j.bspc.٢٠٢١,١٠٣٠٠١.

[٢٨] K. M. Malayeri AB, "Concatenated convolutional neural network model for cufless blood pressure estimation using fuzzy recurrence properties of PPG signals," *Sci Rep*, vol. ١٢: ٦٦٣٣, ٢٠٢٢.

[٢٩] H. L. Hsu Y-C, Li Y-H, Chang C-C, "Generalized deep neural network model for cufess blood pressure estimation with photoplethysmogram signal only," *Sensors*, vol. ٢٠, no. ١٩, p. ٥٦٦٨, ٢٠٢٠.

[٣٠] C. X. Cheng J, Xu Y, Song R, Liu Y, Li C, "Prediction of arterial blood pressure waveforms from photoplethysmogram signals via fully convolutional neural networks," *Comput Biol Med*, vol. ١٣٨:١٠٤٨٧٧, ٢٠٢١.

[٣١] H. W. Li Z, "A continuous blood pressure estimation method using photoplethysmography by GRNNbased model.," *Sensors*, vol. ٢١, no. ٢١, p. ٧٢٠٧, ٢٠٢١.

[٣٢] L. Y.-H. Harfya LN, Chang C-C, "Continuous blood pressure estimation using exclusively photopletysmography by LSTM-based signal-to-signal translation," *Sensors*, vol. ٢١, no. ٩, p. ٢٩٥٢, ٢٠٢١.

[٣٣] C. C.-C. Li Y-H, Harfya LN, "Featureless blood pressure estimation based on photoplethysmography signal using CNN and BiLSTM for IoT devices," *Wirel Commun Mob Comput*, vol. ٢٠٢١, ٢٠٢١.